



**HAL**  
open science

## Zero-contours in low-energy $K$ - $\pi$ scattering

Alain Arnéodo

► **To cite this version:**

Alain Arnéodo. Zero-contours in low-energy  $K$ - $\pi$  scattering. *Il Nuovo Cimento A*, 1975, 25 (3), pp.511-533. 10.1007/bf02820862 . hal-01557180

**HAL Id: hal-01557180**

**<https://hal.science/hal-01557180>**

Submitted on 5 Jul 2017

**HAL** is a multi-disciplinary open access archive for the deposit and dissemination of scientific research documents, whether they are published or not. The documents may come from teaching and research institutions in France or abroad, or from public or private research centers.

L'archive ouverte pluridisciplinaire **HAL**, est destinée au dépôt et à la diffusion de documents scientifiques de niveau recherche, publiés ou non, émanant des établissements d'enseignement et de recherche français ou étrangers, des laboratoires publics ou privés.



Distributed under a Creative Commons Attribution 4.0 International License

# Zero-Contours in Low-Energy K- $\pi$ Scattering.

A. ARNEODO

*Physique Théorique, Université, de Nice - Nice* (\*)(\*\*)

**Summary.** — The paths of zeros of the low-energy K- $\pi$  scattering amplitudes  $A_{s=2}^{I=2}$  and  $A_{s=1}^{I=1}$  are examined in a simple K\* and  $\rho$  dominance model, where it is found that the roles of PCAC zero, K\* and  $\rho$  Legendre zero, and double-pole-killing zero are played by the same zero-contour in the  $(s, t, u)$ -plane, an ellipse for the first amplitude, an ellipse plus the line  $s = u$  for the second one. The behaviour of these zero-contours in the  $u$ -channel physical region is studied in comparison with the experimental zeros determined from the  $K^+\pi^- \rightarrow K^+\pi^-$  and  $K^+\pi^0 \rightarrow K^0\pi^+$  scattering results, and it is found that up to the K\* mass region the elliptic contour of  $A_{s=2}^{I=2}$  is essentially unaffected by unitarity, whilst the elliptic contour of  $A_{s=1}^{I=1}$  is slightly more sensitive to such constraints. A comparison with the behaviour of the zeros of the corresponding  $\pi$ - $\pi$  amplitudes  $A_{\pi\pi}^{I=2}$  and  $A_{\pi\pi}^{I=1}$  is also performed.

## 1. — Introduction.

A few years ago ODORICO has provided a possible explanation of meson-meson scattering data in terms of a hypothesis of a global structure for the straight-line propagation of nearby zeros of the scattering amplitude, whereby lines passing through the intersections of resonances in different channels also pass through the Legendre zeros of resonances in the physical regions of the  $(s, t, u)$ -plane <sup>(1-3)</sup>.

---

(\*) Equipe de Recherche Associée au C.N.R.S.

(\*\*) Postal address: Physique Théorique, I.M.S.P. Parc Valrose, 06034 Nice Cedex.

(<sup>1</sup>) R. ODORICO: *Nucl. Phys.*, **37** B, 509 (1971).

(<sup>2</sup>) R. ODORICO: *Phys. Lett.*, **38** B, 37 (1972).

(<sup>3</sup>) R. ODORICO: *Phys. Lett.*, **38** B, 411 (1972).

Since then numerous studies of zero-contours of the  $\pi$ - $\pi$  scattering amplitude have been performed using the experimental phase shifts (<sup>4,7</sup>). Several of them disagree with certain predictions made by ODORICO, such as for example the analyses of PENNINGTON and PROTOPODESCU (<sup>4</sup>) and of EGUCHI *et al.* (<sup>5</sup>) which contest the suggestion that the anomalous behaviour of the experimental moment  $\langle Y_1^0 \rangle$  at 0.98 GeV may be seen as a consequence of the entry in the physical region of a zero at fixed  $s = 4\mu^2 - 2m_\rho^2$ . Nevertheless on the whole these studies find this straight-line zero hypothesis as a reasonable approximation to reality when viewing the Mandelstam plane from afar. However in any local region zero-contours are far from straight, and this is especially evident in the low-energy region as is discussed by PENNINGTON and SCHMID in ref. (<sup>8</sup>). The theoretical analysis of ARNEODO, GUERIN and DONOHUE (<sup>9</sup>) is also very significant of this feature since it emphasizes that, in a simple nonunitary  $\rho$  dominance model, the nearby zero-contours of low-energy  $\pi$ - $\pi$  scattering amplitudes  $A_{\pi\pi}(s, t, u)$  and  $A_{\pi\pi}^{I, s=2}(s, t, u)$  form a closed curve: a circle in the  $(s, t, u)$ -plane. This circle plays the respective roles of PCAC zero,  $\rho$  Legendre zero and double-pole-killing zero, and is in large part rather stable when unitarity is enforced.

Such experimental and theoretical studies have not been performed in  $K$ - $\pi$  scattering. Thus we propose in this article to examine the behaviour of the zero-contours of the low-energy  $K$ - $\pi$  amplitudes; first in a pure  $K^*$  and  $\rho$  dominance model, which is a model for the whole amplitude and consequently permits us to define the zero-contours in the unphysical as well as the physical regions; then as determined from the experimental phase shift analyses of the reactions  $K^+\pi^- \rightarrow K^+\pi^-$  and  $K^+\pi^0 \rightarrow K^0\pi^+$  (<sup>10-13</sup>), *i.e.* only in particular physical

(<sup>4</sup>) M. R. PENNINGTON and S. D. PROTOPODESCU: *Phys. Lett.*, **40** B, 105 (1972).

(<sup>5</sup>) T. EGUCHI, M. FUKUGITA and T. SHIMADA: *Phys. Lett.*, **48** B, 56 (1973).

(<sup>6</sup>) P. EASTABROOKS, A. D. MARTIN, G. GRAYER, B. HYAMS, C. JONES, P. WEILHAMMER, W. BLUM, H. DIETL, W. KOCH, E. LORENZ, G. LÜTJENS, W. MÄNNER, J. MEISSBURGER and U. STIERLIN: *Conference on  $\pi$ - $\pi$  Scattering, 1973, Tallahassee Conference (A.I.P. Conference Proceedings, No. 13)*.

(<sup>7</sup>) B. HYAMS, C. JONES, P. WEILHAMMER, W. BLUM, H. DIETL, G. GRAYER, W. KOCH, E. LORENZ, G. LÜTJENS, W. MÄNNER, J. MEISSBURGER, W. OCHS, U. STIERLIN and F. WAGNER: *Nucl. Phys.*, **64** B, 134 (1973).

(<sup>8</sup>) M. R. PENNINGTON and C. SCHMID: *Phys. Rev. D*, **7**, 2213 (1973).

(<sup>9</sup>) A. ARNEODO, F. GUERIN and J. T. DONOHUE: *Nuovo Cimento*, **17** A, 329 (1973).

(<sup>10</sup>) R. MERCER, P. ANTICH, A. CALLAHAN, C. Y. CHIEN, B. COX, R. CARSON, D. DENEGRI, L. ETTLINGER, D. FEIOCK, G. GOODMAN, J. HAYNES, A. PEVSNER, R. SEKULIN, V. SREEDHAR and R. ZDANIS: *Nucl. Phys.*, **32** B, 381 (1971).

(<sup>11</sup>) H. H. BINGHAM, W. M. DUNWOODIE, D. DRIJARD, D. LINGLIN, Y. GOLDSCHMIDT-CLERMONT, F. MULLER, T. TRIPPE, F. GRARD, P. HERQUET, J. NAISSE, R. WINDMOLDERS, E. COLTON, P. E. SCHLEIN and W. E. SLATER: *Nucl. Phys.*, **41** B, 1 (1972).

(<sup>12</sup>) A. FIRESTONE, G. GOLDHABER, D. LISSAUER and G. H. TRILLING: *Phys. Rev. D*, **5**, 2188 (1972).

(<sup>13</sup>) S. L. BAKER, S. BANERJEE, J. R. CAMPBELL, G. HALL, A. K. M. A. ISLAM, G. MAY,

regions. For our technical way of describing zero-contours we explicitly refer to the theoretical analysis of ref. (9).

The main result of our investigation is that, in the narrow-width  $K^*$  and  $\rho$  dominance approximation, the zero-contours of the  $K\text{-}\pi$  amplitudes  $A^{I_s=\frac{3}{2}}$  and  $A^{I_s=1}$  are respectively an ellipse and an ellipse plus the line  $s = u$  in the  $(s, t, u)$ -plane. These contours are related to the different zeros arising at low energy: the Adler-Weinberg zero, the Legendre zero of  $K^*$  and  $\rho$  mesons and the double-pole-killing zeros. Moreover the behaviour of the experimental complex zeros suggests that in the low-energy  $u$ -channel physical region ( $u \lesssim m_{K^*}^2$ ) the elliptic zero-contour of the amplitude  $A^{I_s=\frac{3}{2}}$  is essentially unmodified by the unitarity constraints, while the elliptic zero-contour of the amplitude  $A^{I_s=1}$  is more sensitive to unitarization and is drawn into a somewhat straight shape lying at  $t \simeq -0.2 (\text{GeV})^2$ . This simple  $K^*$  and  $\rho$  dominance model is found to be unreliable for energies above 0.95 GeV, since it predicts nearby zero-contours for the both  $K\text{-}\pi$  scattering amplitudes while experimentally the zeros appear to be far away in the complex  $(s, u)$ -space, and consequently the term zero-contour is ambiguous at such energies.

We organize the paper as follows. In Sect. 2 we examine the zero-contours of the simple  $K^*$  and  $\rho$  dominance model. In Sect. 3 we discuss how they are influenced in the  $K^*$  mass region by the unitarity constraints. In Sect. 4 we compare them with the zero-contours calculated from the experimental phase shifts. In Sect. 5 we perform a comparison of zero-contours in  $\pi\text{-}\pi$  and  $K\text{-}\pi$  scattering. Kinematics and amplitudes in  $K\text{-}\pi$  scattering are defined in the Appendix.

## 2. - Zero-contours in the simple Breit-Wigner model.

The contribution of both  $\rho$  and  $K^*$  resonances to the  $K\text{-}\pi$  scattering amplitudes  $A(s, t, u)$  and  $B(s, t, u)$ , which respectively represent in the  $s$ -channel physical region the reactions  $K^+\pi^+ \rightarrow K^+\pi^+$  and  $K^+\pi^- \rightarrow K^0\pi^0$ , may be written in the Breit-Wigner approximation as

$$(2.1) \quad A(s, t, u) = A^{I_s=\frac{3}{2}}(s, t, u) = -\frac{g_\rho}{2} \frac{(s-u)}{D_\rho(t)} + g_{K^*} \frac{[(t-s) + (m^2 - \mu^2)^2/m_{K^*}^2]}{D_{K^*}(u)}$$

---

D. B. MILLER, J. E. ALLEN, P. V. MARCH, S. H. MORRIS, K. O BRIEN and C. E. PEACH:  
*A study of  $K^+\pi^-$  elastic scattering in the reaction  $K^+n \rightarrow K^+\pi^-p$  between 2.0 and 3.0 GeV/c,*  
 submitted to the *II Aix en Provence International Conference on Elementary Particles*  
 (September 1973).

and

$$(2.2) \quad B(s, t, u) = -\frac{1}{\sqrt{2}} A_{I=1}(s, t, u) = \frac{1}{\sqrt{2}} \left\{ -g_\rho \frac{(s-u)}{D_\rho(t)} + g_{\mathbf{K}^*} \left( \frac{(t-s) + (m^2 - \mu^2)^2/m_{\mathbf{K}^*}^2}{D_{\mathbf{K}^*}(u)} - \frac{(t-u) + (m^2 - \mu^2)^2/m_{\mathbf{K}^*}^2}{D_{\mathbf{K}^*}(s)} \right) \right\},$$

with

$$(2.3) \quad \left\{ \begin{array}{l} g_\rho = -\frac{3m_\rho^2 \Gamma_\rho}{4q_\rho^3}, \quad g_{\mathbf{K}^*} = -\frac{4m_{\mathbf{K}^*}^5 \Gamma_{\mathbf{K}^*}}{(m_{\mathbf{K}^*}^2 - (m + \mu)^2)^{\frac{1}{2}} (m_{\mathbf{K}^*}^2 - (m - \mu)^2)^{\frac{1}{2}}} \\ q_\rho = \frac{1}{2} (m_\rho^2 - 4\mu^2)^{\frac{1}{2}}, \quad q_{\mathbf{K}^*} = \frac{1}{2} (m_{\mathbf{K}^*}^2 - (m + \mu)^2)^{\frac{1}{2}}, \\ q_t = \frac{1}{2} (4\mu^2 - t)^{\frac{1}{2}}, \quad q_s = \frac{1}{2} ((m + \mu)^2 - s)^{\frac{1}{2}}, \quad q_u = \frac{1}{2} ((m + \mu)^2 - u)^{\frac{1}{2}}, \\ D_\rho(t) = t - m_\rho^2 - m_\rho \Gamma_\rho \frac{q_t}{q_\rho}, \quad D_{\mathbf{K}^*}(s) = s - m_{\mathbf{K}^*}^2 - m_{\mathbf{K}^*} \Gamma_{\mathbf{K}^*} \frac{q_s}{q_{\mathbf{K}^*}}, \\ D_{\mathbf{K}^*}(u) = u - m_{\mathbf{K}^*}^2 - m_{\mathbf{K}^*} \Gamma_{\mathbf{K}^*} \frac{q_u}{q_{\mathbf{K}^*}}, \end{array} \right.$$

and where it is explicitly assumed that the  $\rho$  couples in the same way to the  $\pi\pi$  and  $\mathbf{K}\bar{\mathbf{K}}$  channels. The respective kaon and pion mass are  $m$  and  $\mu$ , and the details of the  $\mathbf{K}\pi$  kinematics are defined in the Appendix.

This simple model for the low-energy region has the analytic structure needed to incorporate the cuts due to elastic unitarity, but it has no cuts corresponding to inelastic unitarity. One can justify this absence of double-spectral function in so far as the inelastic effects are unimportant, *i.e.* up to 1 GeV (\*). Moreover this model gives the correct threshold behaviour for the real parts of all  $\mathbf{K}\pi$  partial-wave amplitudes, and whilst one cannot determine the scattering amplitudes everywhere, this nonunitary approximation may be considered as reasonable in the low-energy region. (Some problems arising from the incorrect behaviour of the imaginary part of the  $\mathbf{K}\pi$  partial-wave amplitudes will be discussed later.)

In the limit of narrow-width resonances:  $\Gamma_{\mathbf{K}^*}$  and  $\Gamma_\rho$  small, both amplitudes  $A(s, t, u)$  and  $B(s, t, u)$  are real except at  $t = m_\rho^2$ ,  $u = m_{\mathbf{K}^*}^2$  and  $s = m_{\mathbf{K}^*}^2$  (only for  $B(s, t, u)$ ), and the respective zero-surfaces intersect the real  $(s, t, u)$ -plane along the curves defined by

$$(2.4) \quad g_{\mathbf{K}^*} \left[ (t-s) + \frac{(m^2 - \mu^2)^2}{m_{\mathbf{K}^*}^2} \right] (t - m_\rho^2) - \frac{g_\rho}{2} (s-u)(u - m_{\mathbf{K}^*}^2) = 0$$

---

(\*) Specifically, this model does not contain the singularity at  $t = 4m^2$ .

for  $A(s, t, u)$  and

$$(2.5) \quad (s - u) \cdot$$

$$\cdot \left[ g_{\mathbf{K}^*} (t - m_\rho^2) \left( 2t - 2(m^2 + \mu^2) + m_{\mathbf{K}^*}^2 + \frac{(m^2 - \mu^2)^2}{m_{\mathbf{K}^*}^2} \right) - g_\rho (u - m_{\mathbf{K}^*}^2) (s - m_{\mathbf{K}^*}^2) \right] = 0$$

for  $B(s, t, u)$ . For physical mass and width of the meson resonances ( $m_\rho = 0.765$  GeV,  $\Gamma_\rho = 0.135$  GeV and  $m_{\mathbf{K}^*} = 0.890$  GeV,  $\Gamma_{\mathbf{K}^*} = 0.050$  GeV) the re-

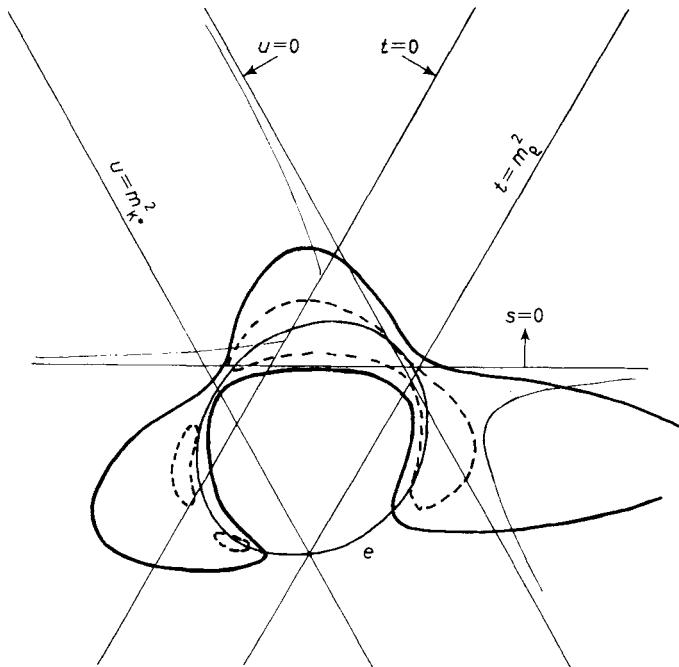


Fig. 1. – Modulus contours of the  $\mathbf{K}\text{-}\pi$  amplitude  $A(s, t, u)$  in the  $(s + i0, t - i0, u + i0)$  limit (see the Appendix for the definition of the limit). The continuous line is  $|A|=1$ , the dashed line  $|A|=0.5$ . The ellipse  $e$  is the zero-contour of the narrow-width approximation of the  $\mathbf{K}^*$  and  $\rho$  dominance model.

lation (2.4) is the equation of an ellipse passing through the  $\rho$  Legendre zero in the  $t$ -channel, the  $\mathbf{K}^*$  Legendre zero in the  $u$ -channel physical region and through the  $\mathbf{K}^*\text{-}\rho$  intersection (Fig. 1). From (2.5) the zero-contour of  $B(s, t, u)$  consists of the line  $s = u$  (which attests to the antisymmetry of this amplitude under the exchange  $s \leftrightarrow u$ ), plus an ellipse passing through the Legendre zero

of the  $K^*$  in the  $s$ - and  $u$ -channel physical regions and through the  $K^*-\rho$  intersections (Fig. 2) (\*).

When  $\Gamma_{K^*}$  and  $\Gamma_\rho$  are not very small, one expects these curves of nearest zeros to have moved to complex values of  $s$  and  $u$ , except in the region  $\{t \leq 4\mu^2, s \leq (m + \mu)^2, u \leq (m + \mu)^2\}$  where the amplitudes  $A(s, t, u)$  and  $B(s, t, u)$  are real.

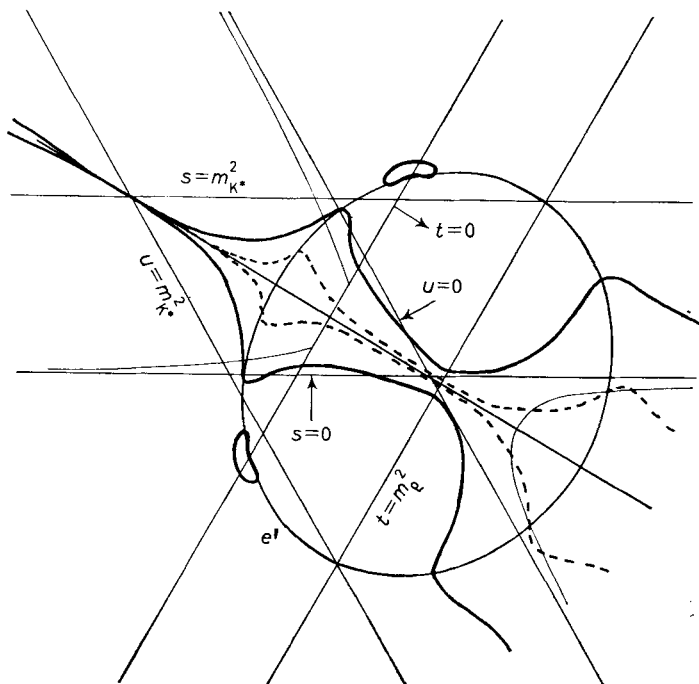


Fig. 2. - Modulus contours of the  $K-\pi$  amplitude  $B(s, t, u)$  in the  $(s + i0, t + i0, u + i0)$  limit. The continuous line is  $|B|=1$ , the dashed line  $|B|=0.2$ . The zero-contour predictions of the narrow-width  $K^*$  and  $\rho$  dominance model consist of the line  $s = u$ , plus the ellipse  $e'$ .

Before developing this study of complex zeros we must resolve a problem inherent in this simple Breit-Wigner model which consists in an incorrect behaviour of the imaginary part of the  $I = \frac{1}{2}$   $K-\pi$   $S$ -wave amplitude. If, on the one hand, the expressions (2.1) and (2.2) do not give a correct threshold behaviour for the imaginary parts of the partial-wave amplitudes, on the other hand they

(\*) In the model based on Lagrangian theory of D. IAGOLNITZER *et al.* (14), where  $SU_3$  symmetry is broken by mass terms, the values of mass and width of the resonances  $\rho$  and  $K^*$  obey the relation  $g_\rho = 2g_{K^*}$ . In this case the zero-contours of  $A(s, t, u)$  and  $B(s, t, u)$  defined by (2.4) and (2.5) are circles passing through the same points previously defined for the ellipses.

(14) D. IAGOLNITZER, J. ZINN-JUSTIN and J. B. ZUBER: *Nucl. Phys.*, **60** B, 233 (1973).

imply more dramatically that the imaginary part of the  $I = \frac{1}{2}$   $S$ -wave is negative, though quite small ( $< 0.06$ ), up to the  $K^*$  mass. In order to eliminate this difficulty we added linear terms in  $q_s$ ,  $q_t$  and  $q_u$  to the simple Breit-Wigner approximation to the  $K$ - $\pi$  amplitudes

$$(2.6) \quad A(s, t, u) = A_{\text{BW}}(s, t, u) + (\alpha - \beta)q_s + (\alpha + \beta)q_u + \gamma q_t$$

and

$$(2.7) \quad B(s, t, u) = B_{\text{BW}}(s, t, u) + \sqrt{2}\beta(q_u - q_s)$$

where  $A_{\text{BW}}(s, t, u)$  and  $B_{\text{BW}}(s, t, u)$  are given by the expressions (2.1) and (2.2), and  $\alpha$ ,  $\beta$ ,  $\gamma$  are parameters. We fixed these parameters by imposing the unitarity constraints at threshold in the  $s$ - and  $t$ -channels. In the  $s$ -channel we have

$$(2.8) \quad \lim_{s \rightarrow (m+\mu)^2} \left[ \frac{\text{Im } f'_0(s)}{Q(s)} \right] = (m + \mu)(a'_0)^2,$$

where  $f'_0(s)$  are the  $S$ -wave amplitudes ( $I = \frac{1}{2}$  or  $\frac{3}{2}$ ) defined from (2.6) and (2.7) (see the Appendix), and  $a'_0$  the corresponding scattering lengths. In the  $t$ -channel we have

$$(2.9) \quad \lim_{t \rightarrow 4\mu^2} \left[ \frac{\text{Im } T_0^0(t)}{Q(t)} \right] = \Pi_0^0 \text{Re } T_0^0(4\mu^2),$$

where  $T_0^0(t)$  is defined in the Appendix and  $\Pi_0^0$  is the  $I = 0$   $S$ -wave scattering length of the  $\pi$ - $\pi$  amplitude. In the following we shall consider  $\Pi_0^0$  to be equal to  $0.17\mu^{-1}$ , and we shall discuss the importance of this choice at the end of this Section. We then find that  $\alpha = -0.575 (\text{GeV})^{-1}$ ,  $\beta = 0.078 (\text{GeV})^{-1}$ ,  $\gamma = 0.875 (\text{GeV})^{-1}$ , whereas the  $K\pi$   $S$ -wave scattering lengths turn out to be  $a_0^{\frac{1}{2}} = 0.11\mu^{-1}$  and  $a_0^{\frac{3}{2}} = -0.15\mu^{-1}$ . These values are close to those predicted by current algebra and lie within the band found by ADER *et al.* using crossing, unitarity and the existence of the  $K^*$  <sup>(15,16)</sup>. Moreover the  $I = \frac{1}{2}$   $S$ -wave has a positive imaginary part but is not unitary, except at the threshold from (2.8). Similarly eq. (2.8) makes the  $I = \frac{3}{2}$   $S$ -wave unitary only at threshold. The other partial waves are not unitary even at threshold.

Now, having resolved the important problem of the positivity of the imaginary part of the  $I = \frac{1}{2}$   $S$ -wave (but not the general problem of unitarity), we are allowed to define the complex zeros of the  $K$ - $\pi$  scattering amplitudes.

<sup>(15)</sup> J. P. ADER, C. MEYERS and B. BONNIER: *Nucl. Phys.*, **45** B, 554 (1972).

<sup>(16)</sup> J. P. ADER, C. MEYERS and B. BONNIER: *Phys. Lett.*, **46** B, 403 (1973).

**2'1. Complex zeros of  $A(s, t, u)$ .** – From (2.6) the zeros of the amplitude  $A(s, t, u)$  are given by

$$(2.10) \quad g_{\mathbf{K}^*} \left[ (t-s) + \frac{(m^2 - \mu^2)^2}{m_{\mathbf{K}^*}^2} \right] D_\rho(t) - \frac{g_\rho}{2} (s-u) D_{\mathbf{K}^*}(u) + \\ + [(\alpha - \beta)q_s + (\alpha + \beta)q_u + \gamma q_t] D_\rho(t) D_{\mathbf{K}^*}(u) = 0 ,$$

which defines a two-dimensional surface in the complex  $(s, u)$ -space. The following points lie on this surface:

$$\begin{aligned} \text{i) } \quad & s = u , \quad t = m_\rho^2 \left( 1 - \frac{\Gamma_\rho^2}{8q_\rho^2} \right) - im_\rho \Gamma_\rho \left[ 1 - \left( \frac{m_\rho \Gamma_\rho}{8q_\rho^2} \right)^2 \right]^{\frac{1}{2}} ; \\ \text{ii) } \quad & s = t + \frac{(m^2 - \mu^2)^2}{m_{\mathbf{K}^*}^2} , \\ & u = m_{\mathbf{K}^*}^2 \left( 1 - \frac{\Gamma_{\mathbf{K}^*}^2}{8q_{\mathbf{K}^*}^2} \right) - im_{\mathbf{K}^*} \Gamma_{\mathbf{K}^*} \left[ 1 - \left( \frac{m_{\mathbf{K}^*} \Gamma_{\mathbf{K}^*}}{8q_{\mathbf{K}^*}^2} \right)^2 \right]^{\frac{1}{2}} ; \\ \text{iii) } \quad & t = m_\rho^2 \left( 1 - \frac{\Gamma_\rho^2}{8q_\rho^2} \right) - im_\rho \Gamma_\rho \left[ 1 - \left( \frac{m_\rho \Gamma_\rho}{8q_\rho^2} \right)^2 \right]^{\frac{1}{2}} , \\ & u = m_{\mathbf{K}^*}^2 \left( 1 - \frac{\Gamma_{\mathbf{K}^*}^2}{8q_{\mathbf{K}^*}^2} \right) - im_{\mathbf{K}^*} \Gamma_{\mathbf{K}^*} \left[ 1 - \left( \frac{m_{\mathbf{K}^*} \Gamma_{\mathbf{K}^*}}{8q_{\mathbf{K}^*}^2} \right)^2 \right]^{\frac{1}{2}} . \end{aligned}$$

These points may be associated, in this order, with the zero of the Legendre polynomial at the  $\rho$  mass in the  $t$ -channel and at the  $\mathbf{K}^*$  mass in the  $u$ -channel physical region, and the double-pole-killing zero at the intersection of the  $\rho$  and the  $\mathbf{K}^*$ . The projections of these points on the real  $(s, t, u)$ -plane are essentially independent of  $\Gamma_\rho$  and  $\Gamma_{\mathbf{K}^*}$ , provided that  $\Gamma_\rho \ll m_\rho$  and  $\Gamma_{\mathbf{K}^*} \ll m_{\mathbf{K}^*}$ . Their respective distances from this plane are characterized by  $\text{Im } t$  of order  $m_\rho \Gamma_\rho$  and  $\text{Im } u$  of order  $m_{\mathbf{K}^*} \Gamma_{\mathbf{K}^*}$ , hence one expects the zeros of  $A(s, t, u)$  to be nearby zeros. But this generalization is not evident in view of the presence of linear terms in  $q_s$ ,  $q_t$  and  $q_u$  in the expression of  $A(s, t, u)$ . So we traced in Fig. 1 the modulus contours of this amplitude in the real  $(s, t, u)$ -plane. It is clear from this Figure that there exists a curve along which  $A(s, t, u)$  shows a pronounced sharp minimum, and it is reasonable to associate this with a nearby zero-contour as is discussed in ref. (9). Moreover this curve of minimal  $|A|$  is not very different from the elliptic zero-contour of the narrow-width meson resonance approximation. The unitarization procedure at the threshold, defined by (2.8) and (2.9), tends somewhat to draw the original ellipse of zeros into a triangular shape with the horizontal base passing through the  $\mathbf{K}^*$ - $\rho$  intersection, but this effect is indeed not very pronounced. As we have previously remarked, this quasi-elliptic contour of nearby zeros plays the roles of the  $\rho$  Legendre zero, the  $\mathbf{K}^*$  Legendre zero and the  $\mathbf{K}^*$ - $\rho$  crossing zero. In

addition it also plays the role of the Adler-Weinberg zero, since it passes through the real  $(s, t, u)$ -plane region:  $\{t \leq 4\mu^2, s \text{ and } u \leq (m + \mu)^2\}$  not very far from the line  $s = m^2 + \mu^2$ , which corresponds to a smooth extrapolation of the current algebra zero to the on-mass-shell amplitude.

2.2. *Complex zeros of  $B(s, t, u)$ .* – From (2.7) the zeros of the amplitude  $B(s, t, u)$  are given by

$$(2.11) \quad g_{\mathbf{K}^*} D_\rho(t) \cdot \left[ \left( (t-s) + \frac{(m^2 - \mu^2)^2}{m_{\mathbf{K}^*}^2} \right) D_{\mathbf{K}^*}(s) - \left( (t-u) + \frac{(m^2 - \mu^2)^2}{m_{\mathbf{K}^*}^2} \right) D_{\mathbf{K}^*}(u) \right] - [g_\rho(s-u) + 2\beta(q_s - q_u) D_\rho(t)] D_{\mathbf{K}^*}(s) D_{\mathbf{K}^*}(u) = 0,$$

which defines a two-dimensional surface in the complex  $(s, u)$ -space. The following points lie on this surface:

$$\begin{aligned} \text{i)} \quad & u = t + \frac{(m^2 - \mu^2)^2}{m_{\mathbf{K}^*}^2}, \\ & s = m_{\mathbf{K}^*}^2 \left( 1 - \frac{I_{\mathbf{K}^*}^2}{8q_{\mathbf{K}^*}^2} \right) - im_{\mathbf{K}^*} I'_{\mathbf{K}^*} \left[ 1 - \left( \frac{m_{\mathbf{K}^*} I'_{\mathbf{K}^*}}{8q_{\mathbf{K}^*}^2} \right)^2 \right]^{\frac{1}{2}}; \\ \text{ii)} \quad & s = t + \frac{(m^2 - \mu^2)^2}{m_{\mathbf{K}^*}^2}, \\ & u = m_{\mathbf{K}^*}^2 \left( 1 - \frac{I_{\mathbf{K}^*}^2}{8q_{\mathbf{K}^*}^2} \right) - im_{\mathbf{K}^*} I'_{\mathbf{K}^*} \left[ 1 - \left( \frac{m_{\mathbf{K}^*} I'_{\mathbf{K}^*}}{8q_{\mathbf{K}^*}^2} \right)^2 \right]^{\frac{1}{2}}; \\ \text{iii)} \quad & s = u, \\ & t = m_\rho^2 \left( 1 - \frac{I_\rho^2}{8q_\rho^2} \right) - im_\rho I'_\rho \left[ 1 - \left( \frac{m_\rho I'_\rho}{8q_\rho^2} \right)^2 \right]^{\frac{1}{2}}; \\ \text{iv)} \quad & t = m_\rho^2 \left( 1 - \frac{I_\rho^2}{8q_\rho^2} \right) - im_\rho I'_\rho \left[ 1 - \left( \frac{m_\rho I'_\rho}{8q_\rho^2} \right)^2 \right]^{\frac{1}{2}}, \\ & s \text{ (or } u) = m_{\mathbf{K}^*}^2 \left( 1 - \frac{I_{\mathbf{K}^*}^2}{8q_{\mathbf{K}^*}^2} \right) - im_{\mathbf{K}^*} I'_{\mathbf{K}^*} \left[ 1 - \left( \frac{m_{\mathbf{K}^*} I'_{\mathbf{K}^*}}{8q_{\mathbf{K}^*}^2} \right)^2 \right]^{\frac{1}{2}}; \\ \text{v)} \quad & s = u = m_{\mathbf{K}^*}^2 \left( 1 - \frac{I_{\mathbf{K}^*}^2}{8q_{\mathbf{K}^*}^2} \right) - im_{\mathbf{K}^*} I'_{\mathbf{K}^*} \left[ 1 - \left( \frac{m_{\mathbf{K}^*} I'_{\mathbf{K}^*}}{8q_{\mathbf{K}^*}^2} \right)^2 \right]^{\frac{1}{2}}. \end{aligned}$$

These points correspond respectively to the  $\mathbf{K}^*$  Legendre zero in the  $s$ - and  $u$ -channel physical regions, the  $\rho$  Legendre zero in the  $t$ -channel and to the double-pole-killing zero at the  $\mathbf{K}^*-\rho$  and  $\mathbf{K}^*-\mathbf{K}^*$  intersections. They exhibit the same features as the previously described points of the zero-surface of  $am$ .

plitude  $A(s, t, u)$ . In the same way the modulus contours of the amplitude  $B(s, t, u)$  attest to the existence of a nearby zero-contour, which is characterized by a curve (plus a line) of minimal  $|B|$  lying very close to the ellipse (the line  $s = u$ ) of the original narrow-width meson resonance model (Fig. 2). Consequently the unitarization procedure at the threshold defined by (2.8) and (2.9) does not greatly disturb the behaviour of the zero-contour of  $B(s, t, u)$ . This result is easily explained by the small value taken by the  $\beta$ -parameter ( $= 0.078 \text{ (GeV)}^{-1}$ ).

To conclude this description we want to discuss the sensitivity of the paths of zeros of the amplitudes  $A(s, t, u)$  and  $B(s, t, u)$  to the value of the  $I = 0$   $\pi\pi$   $S$ -wave scattering length  $\Pi_0^0$  injected in the unitarity constraint at the threshold in the  $t$ -channel (2.9). Previously this scattering length took the value given by the current algebra theory and the zero-contours lay very close to the elliptic forms given by the narrow-width resonance approximation. Now if  $\Pi_0^0$  takes values in a domain which is compatible with the current algebra predictions (for example  $0.07\mu^{-1} < \Pi_0^0 < 0.27\mu^{-1}$ ), the behaviour of the zero-contours is essentially independent of the value chosen. In particular the paths of zeros associated with the value of  $\Pi_0^0$  found in the model of ref. (17,18) ( $\Pi_0^0 \simeq 0.095\mu^{-1}$ ) are in perfect agreement with the ellipses of zeros defined by eqs. (2.4) and (2.5). Now if  $\Pi_0^0$  takes values which are significantly different from the current algebra value, e.g. the value  $\Pi_0^0 = 0.6\mu^{-1}$  predicted by the experimental results on the low-energy  $\pi^0\text{-}\pi^0$  (19,20) and  $K_{e4}$  (21,22), the zero-contours are strongly affected by such a choice (the  $\alpha$ ,  $\beta$  and  $\gamma$  parameters become important). Thus the original elliptic shape of the zero-contours is distorted, in particular for the amplitude  $A(s, t, u)$ . Moreover the zero-surfaces go away from the real  $(s, t, u)$ -plane in certain regions such as the  $u$ -channel physical region of the two amplitudes  $A(s, t, u)$  and  $B(s, t, u)$ , where they respectively represent the experimentally well-known reactions  $K^+\pi^- \rightarrow K^+\pi^-$  and  $K^+\pi^0 \rightarrow K^0\pi^+$ , and the definition of the zero-contours becomes ambiguous. Therefore it appears clear that in a low-energy Breit-Wigner picture of the  $K$ - $\pi$  am-

(17) F. ARBAB and J. T. DONOHUE: *Phys. Rev. D*, **1**, 217 (1970).

(18) A. ARNEODO and J. T. DONOHUE: *Nuovo Cimento*, **15 A**, 107 (1973).

(19) J. R. BENSINGER, A. R. ERWIN, M. A. THOMPSON and W. D. WALKER: *Phys. Lett.* **36 B**, 134 (1971).

(20) P. SONDEREGGER and P. BONAMY: *Proceedings of the Fifth International Conference on Elementary Particles, Lund, 1969* (Paper No. 732, unpublished).

(21) A. ZYLBERSZTEJN, P. BASILE, M. BOURQUIN, J. P. BOYMOND, A. DIAMANT-BERGER, P. EXTERMANN, P. KUNZ, R. MERMOD, H. SUTER and R. TURLAY: *Phys. Lett.*, **38 B**, 457 (1972).

(22) G. VILLET, M. DAVID, R. AYED, P. BAREYRE, P. BORGEAUD, J. ERNWEIN, J. FELTESSE, Y. LEMOIGNE, P. MARTY and A. V. STIRLING: *Conference on  $\pi$ - $\pi$  Scattering, 1973, Tallahassee Conference (A.I.P. Conference Proceedings, No. 13)*.

plitudes the zero-contours are stable features against the unitarization procedure at the threshold (in the three channels) only so long the  $I = 0$   $\pi\text{-}\pi$   $S$ -wave scattering length is compatible with the current algebra predictions.

### 3. – Zero-contours in the $K^*$ region and unitarity constraints.

In order to investigate the consequences of unitarity for the nearby zero-contours, we transpose the analysis which PENNINGTON and SCHMID have performed for  $\pi\text{-}\pi$  scattering<sup>(8)</sup> to the case of  $K\text{-}\pi$  scattering.

In the  $u$ -channel physical region of the  $K\text{-}\pi$  amplitude  $A(s, t, u)$ , only the  $S$  and  $P$  waves are important near the  $K^*$  resonance. Hence the equation of zeros

$$A(s, t, u) = \frac{1}{3} (A^{I=0}(u, t, s) + 2A^{I=1}(u, t, s)) = 0$$

may be written as

$$(3.1) \quad (f_1^{\frac{3}{2}}(u) + 2f_1^{\frac{1}{2}}(u)) \cos \theta^*(u) + \frac{1}{3} (f_0^{\frac{3}{2}}(u) + 2f_0^{\frac{1}{2}}(u)) = 0.$$

Moreover in the  $K^*$  region we can reasonably neglect the  $I = \frac{3}{2}$   $P$ -wave and represent the  $I = \frac{1}{2}$   $P$ -wave by a unitary Breit-Wigner form. Using a phase shift representation for the  $S$ -waves, we obtain for the projection of the nearby complex zeros onto the real  $(s, t, u)$ -plane

$$(3.2) \quad \text{Re}(\cos \theta^*(u)) = -\frac{1}{6} \left[ \frac{m_{K^*}^2 - u}{2m_{K^*} I_{K^*}} (\sin 2\delta_0^{\frac{3}{2}}(u) + 2 \sin 2\delta_0^{\frac{1}{2}}(u)) + (\sin^2 \delta_0^{\frac{3}{2}}(u) + 2 \sin^2 \delta_0^{\frac{1}{2}}(u)) \right].$$

On the line  $u = m_{K^*}^2$  the zero occurs for

$$(3.3) \quad \text{Re}(\cos \theta^*(u = m_{K^*}^2)) = -\frac{1}{6} (\sin^2 \delta_0^{\frac{3}{2}}(m_{K^*}^2) + 2 \sin^2 \delta_0^{\frac{1}{2}}(m_{K^*}^2)),$$

which is proportional to the value taken at the  $K^*$  mass by the imaginary part of the  $S$ -wave amplitude in the  $u$ -channel physical region. This expression implies that the unitarity constraints cannot shift the intercept beyond the following limits:

$$(3.4) \quad -\frac{1}{2} \leq \text{Re}(\cos \theta^*(u = m_{K^*}^2)) \leq 0.$$

Furthermore, if the exotic  $I = \frac{3}{2}$   $S$ -wave is small, the effective lower limit for the intercept is  $\simeq -\frac{1}{3}$ . If one believes in the current algebra zero-contour in the region below threshold in all channels, then the true nearby zero-contour cannot deviate much from that given by the Breit-Wigner model, since it must

intersect the line  $u = m_{\mathbf{K}^*}^2$  between  $-\frac{1}{3}$  and zero. (The Breit-Wigner model predicts an intercept at  $\cos \theta(u) = 0$ .)

If we repeat this analysis for the  $\mathbf{K}\text{-}\pi$  amplitude  $B(s, t, u)$ , we obtain for the projection of the nearby complex zeros onto the real plane in the  $u$ -channel physical region

$$(3.5) \quad \text{Re}(\cos \theta^*(u)) = -\frac{1}{3} \left[ \frac{m_{\mathbf{K}^*}^2 - u}{2m_{\mathbf{K}^*} \Gamma_{\mathbf{K}^*}} (\sin 2\delta_0^{\frac{1}{2}}(u) - \sin 2\delta_0^{\frac{3}{2}}(u)) + (\sin^2 \delta_0^{\frac{1}{2}}(u) - \sin^2 \delta_0^{\frac{3}{2}}(u)) \right].$$

At  $u = m_{\mathbf{K}^*}^2$ , the zero occurs at

$$(3.6) \quad \text{Re}(\cos \theta^*(u = m_{\mathbf{K}^*}^2)) = -\frac{1}{3} (\sin^2 \delta_0^{\frac{1}{2}}(m_{\mathbf{K}^*}^2) - \sin^2 \delta_0^{\frac{3}{2}}(m_{\mathbf{K}^*}^2)).$$

This expression implies that the intercept remains within the unitarity limits

$$(3.7) \quad -\frac{1}{3} \leq \text{Re}(\cos \theta^*(u = m_{\mathbf{K}^*}^2)) \leq \frac{1}{3}.$$

#### 4. - Zero-contours and low-energy $\mathbf{K}\text{-}\pi$ scattering data.

There exist two different methods of describing zero-contours of an amplitude  $A(s, t, u)$ : the contours of minimal modulus and the intersection of the hyperplane  $\text{Im } u = 0$  with the surface  $A(s, t, u) = 0$ . One method, which we employed in our definition of the theoretical paths of zeros of the  $\mathbf{K}\text{-}\pi$  amplitudes in Sect. 2, corresponds experimentally to finding the minimum of the differential cross-sections. The other consists in determining the zero-contours for  $A(s, t, u)$  in the  $u$ -channel using the phase shifts of the dominant waves, which are experimentally accessible; one solves for the complex values of  $\cos \theta^*(u)$  such that  $A(u, \cos \theta^*(u)) = 0$ , and then projects onto the real  $(s, t, u)$ -plane. The respective properties of these two methods are discussed in detail in ref. (9,23). The main result of these analyses is that both methods lead to the same definition of zero-contours if the amplitude possesses nearby zeros, which are illustrated by the existence of a curve (or curves) along which the amplitude shows a pronounced sharp minimum. On the other hand, if the zeros acquire a nonnegligible imaginary part, the modulus contours no longer present such strongly marked features and the definition of zero-contours becomes so ambiguous that the two methods lead to different conclusions. Consequently if one uses the second method of describing the experimental paths

---

(23) M. R. PENNINGTON: *Conference on  $\pi\text{-}\pi$  Scattering, 1973, Tallahassee Conference (A.I.P. Conference Proceedings, No. 13)*.

of zeros, as we propose to do in this Section, we must take into account not only the projection of the complex zeros onto the real  $(s, t, u)$ -plane but also their distance from this plane, *i.e.* the imaginary part of these zeros. Moreover, as it is always interesting to look at what happens in the differential cross-section, we shall do so and compare the eventual minima with the real parts of the complex zeros.

We determine the experimental zeros by using the three following phase shift analyses:

i) The analysis of the  $S$  and  $P$   $K$ - $\pi$  scattering wave phase shifts from threshold to  $m_{K\pi} = 1.2$  GeV made by MERCER *et al.* <sup>(10)</sup>.

ii) The same analysis made by BINGHAM *et al.* with a different method and better statistics <sup>(11)</sup>.

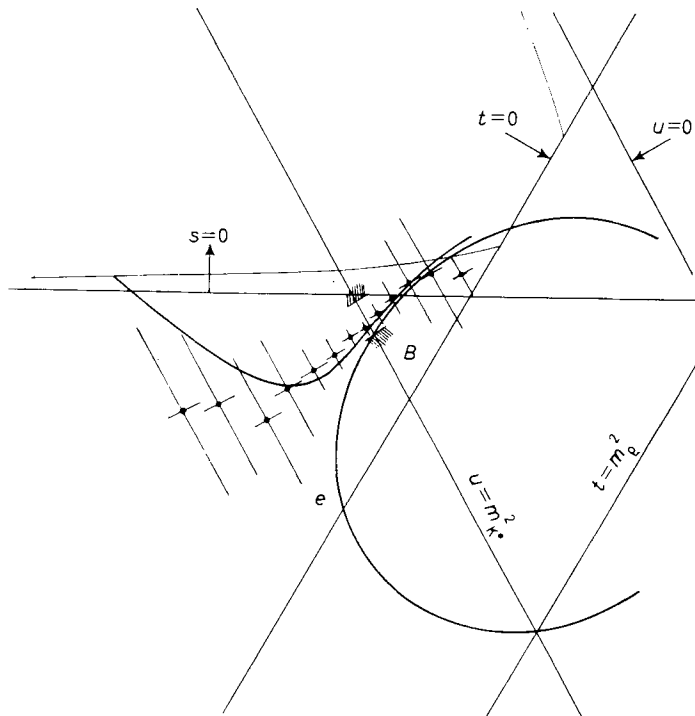


Fig. 3. - The real part of the complex zeros of the  $K$ - $\pi$  amplitude  $\Delta(s, t, u)$  in the  $u$ -channel physical region, where it represents the  $K^+\pi^-$  elastic scattering, as determined from the data of ref. <sup>(10,11)</sup>. The black points are obtained by considering the exact values (with independent errors) of the experimental wave phase shifts of MERCER; the continuous line by considering fits of the wave phase shifts of BINGHAM. The ellipse  $e$  is the zero-contour of the narrow-width approximation of the  $K^*$  and  $\rho$  dominance model. The bounds  $B$  at  $u = m_{K^*}^2$  are the unitarity bounds  $-\frac{1}{2} \leq \text{Re}(\cos \theta^*(u)) < 0$ .

iii) The analysis of  $S$ -,  $P$ - and  $D$ -wave phase shifts in  $K^+\pi^-$  elastic scattering has been performed by FIRESTONE *et al.* <sup>(12)</sup> up to  $m_{K\pi} = 1.7$  GeV, and by BAKER *et al.* <sup>(13)</sup> up to 1.3 GeV. Since the latter find results not very different to those of the former, we shall employ only the FIRESTONE *et al.* results in our search for nearby zeros.

At this point let us remark that the analyses ii) and iii) yield two solutions for the  $I = \frac{1}{2}$   $S$ -wave phase shift. In what follows we use only the «down» solution. The «up» solution resembles the «down» solution except that it

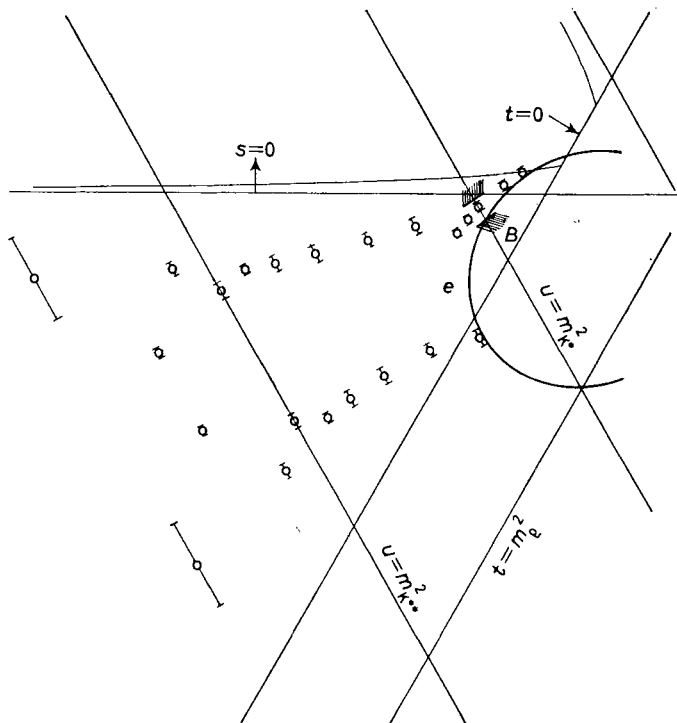


Fig. 4. - The real part of the complex zeros of the  $K\text{-}\pi$  amplitude  $A(s, t, u)$  in the  $u$ -channel physical region as determined from the data of FIRESTONE (ref. <sup>(12)</sup>). The error bars are deduced from experimental errors in the determination of the  $I = \frac{1}{2}$   $S$ -wave phase shift.

has a narrow ( $\leq 30$  MeV) resonance near  $m_{K^*}$ . The zero-contour structures are quite similar for the two solutions except in a very narrow interval near  $u = m_{K^*}^2$ .

We show in Fig. 3 and 4 the real part of the complex zeros of the  $K\text{-}\pi$  scattering amplitude  $A(s, t, u)$  in the  $u$ -channel (where it represents in the physical region the reaction  $K^+\pi^- \rightarrow K^+\pi^-$ ), obtained from the previously quoted experiments. In Fig. 5 is shown the imaginary part of  $\cos \theta^*(u)$ . From these

Figures it is clear that the zero-contour suggested by the Breit-Wigner model is in reasonable agreement with the experimental results for  $u \lesssim m_{\mathbf{K}^*}^2$ . The « first » zero which enters the physical region does this through the backward direction with an imaginary part of  $\cos \theta^*(u) \simeq (-0.3, -0.4)$ , and moves

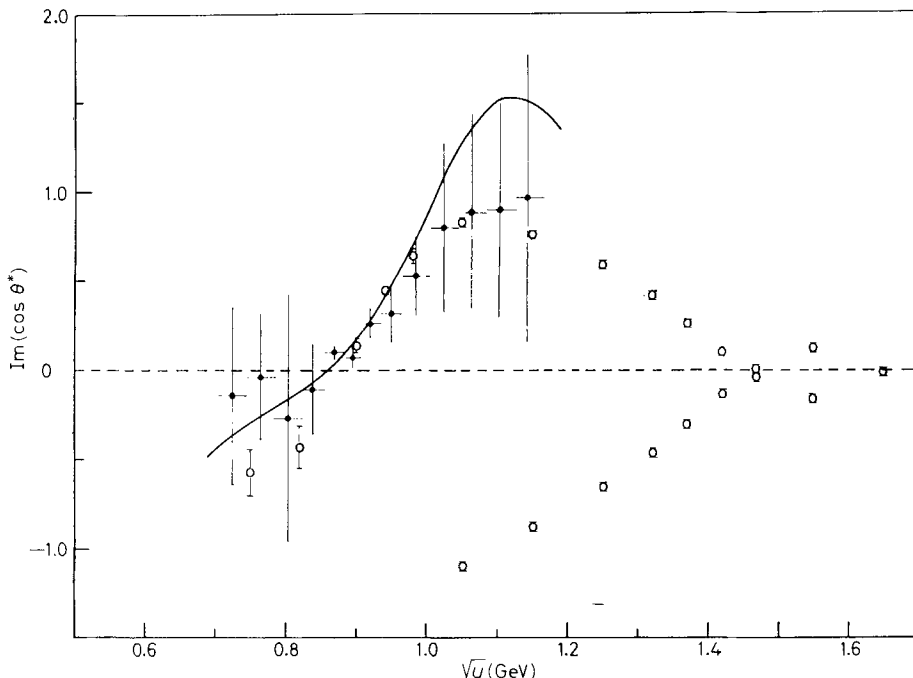


Fig. 5. — The imaginary part of the complex zeros of the  $\mathbf{K}\text{-}\pi$  amplitude  $A(s, t, u)$  in the  $u$ -channel physical region as defined by  $\text{Im} \cos \theta^*(u)$  using the data of MERCER (black points), BINGHAM (continuous line) and FIRESTONE (circles).

smoothly towards the centre of the physical region, lying very close to the ellipse defined by the eq. (2.4). This zero, which is a nearby zero having  $|\text{Im} \cos \theta^*(u)| \lesssim 0.3$  for  $u \lesssim 0.85 (\text{GeV})^2$ , passes in the vicinity of the  $\mathbf{K}^*$  Legendre zero and is associated with a pronounced dip in the differential cross-section. Beyond the  $\mathbf{K}^*$  region the imaginary part of  $\cos \theta^*(u)$  increases rapidly and the projection of this complex zero onto the real  $(s, t, u)$ -plane no longer corresponds to a minimum in the differential cross-section which, indeed, presents a very flat, featureless behaviour at such energies. Near  $u \simeq 1 (\text{GeV})^2$  the  $D$ -wave starts to contribute and a « second » zero begins to approach the physical region. Thus, in this region of higher energies we have to refer to the only  $D$ -wave phase shift analysis, *i.e.* to the Firestone *et al.* experiment (Fig. 4 and 5). As is well known, we cannot determine the zero-contours far outside the physical region since a finite number of partial waves provides a poor rep-

resentation of the amplitude there. Nevertheless we see that this «second» zero enters the physical region through the forward direction at approximately the place predicted by the simple Breit-Wigner model of Sect. 2, and with  $|\text{Im} \cos \theta^*(u)| \simeq 0.9$ . It is not a nearby zero and its entrance in the  $u$ -channel physical region causes the real part of the «first» zero to recoil somewhat towards the backward direction. Then the real part of the «first» zero lines up, ready to become one of the Legendre zeros of the  $\text{K}^{**}(1420)$ -resonance, while the real part of the «second» zero moves, ready to become the other  $\text{K}^{**}$  Legendre zero. At the same time that they approach the  $\text{K}^{**}$  region, these complex zeros approach the real  $(s, t, u)$ -plane and they produce a more and more marked double-dip structure in the differential cross-section. Hence at  $u \simeq m_{\text{K}^{**}}^2$  both zeros are respectively characterized by

$$\text{Re} \cos \theta_1^*(u) \simeq -\text{Re} \cos \theta_2^*(u) \simeq -0.5$$

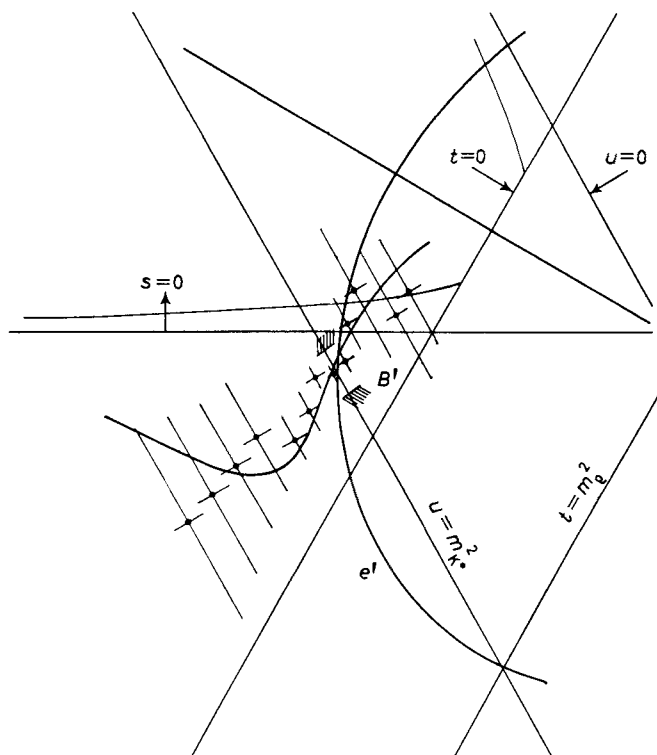


Fig. 6. - The real part of the complex zeros of the  $\text{K}\text{-}\pi$  amplitude  $B(s, t, u)$  in the  $u$ -channel physical region, where it represents the reaction  $\text{K}^+\pi^0 \rightarrow \text{K}^0\pi^+$ , as determined from the data of MERCER (black points) and BINGHAM (continuous line). The ellipse  $e'$  (plus the line  $s = u$ ) is the zero-contour given by the narrow-width approximation of the  $\text{K}^{*-}$  and  $\rho$ -dominance model. The bounds  $B'$  at  $u = m_{\text{K}^{**}}^2$  are the unitarity bounds:  $-\frac{1}{3} \leq \text{Re} \cos \theta^*(u) \leq +\frac{1}{3}$ .

and

$$|\operatorname{Im} \cos \theta_1^*(u)| \simeq |\operatorname{Im} \cos \theta_2^*(u)| \lesssim 0.1.$$

We show in Fig. 6 and 7 the respective real and imaginary parts of the complex zeros of the  $\mathbf{K}$ - $\pi$  scattering amplitude  $B(s, t, u)$  in the  $u$ -channel (where

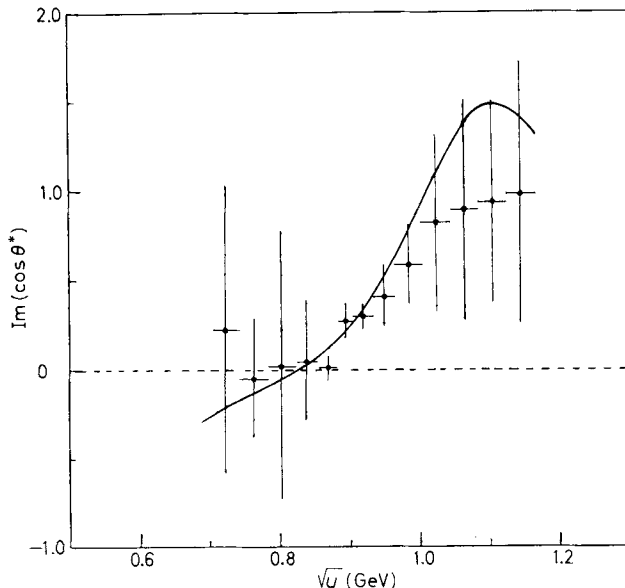


Fig. 7. - The imaginary part of the complex zeros of the  $\mathbf{K}$ - $\pi$  amplitude  $B(s, t, u)$  in the  $u$ -channel physical region as defined by  $\operatorname{Im} \cos \theta^*(u)$  using the data of MERCER (black points) and BINGHAM (circles).

it represents in the physical region the reaction  $\mathbf{K}^+\pi^0 \rightarrow \mathbf{K}^0\pi^+$ ) obtained from the analyses i) and ii) (\*). One can see from these Figures that the deviation from the elliptic contour of the narrow-width  $\mathbf{K}^*$  and  $\rho$  dominance model seems to be more important for this amplitude than for the amplitude  $A(s, t, u)$ . Indeed the zero enters the physical region through the backward direction before the elliptic contour and with a small imaginary part, *e.g.*  $|\operatorname{Im} \cos \theta^*(u)| \simeq \simeq 0.1$ . It moves smoothly towards the centre of the physical region where it crosses the line  $u = m_{\mathbf{K}^*}^2$  very close to  $\cos \theta(u) = 0$ . This zero is a nearby zero having  $|\operatorname{Im} \cos \theta^*(u)| \lesssim 0.3$  for  $u \lesssim 0.85$  (GeV)<sup>2</sup>, and it produces a marked dip in the differential cross-section. As for the amplitude  $A(s, t, u)$ , the zero rapidly goes away in the complex  $(s, u)$ -space beyond this energy and is no longer associated with such a dip structure in the differential cross-section. For  $u \gtrsim \gtrsim 1$  (GeV)<sup>2</sup> the zero described in both Fig. 6 and 7 becomes meaningless since

---

(\*) FIRESTONE *et al.* have analysed only  $\mathbf{K}^+\pi^-$  elastic scattering.

the  $S$ - and  $P$ -waves do not yield a good approximation to the amplitude  $B(s, t, u)$  at such energies. Moreover this lack of  $D$ -wave analysis does not allow us to study the entrance and the behaviour of the double-pole-killing zero in the  $u$ -channel physical region. We remark in addition that the experimental results suggest a possible contour of nearby zeros at  $t \simeq -0.2$  (GeV)<sup>2</sup> for  $A_{\pi\pi}^{I=1}(s, t, u)$ .

Finally for completeness we have tried to define the paths of zeros of the  $K\text{-}\pi$  scattering amplitude  $A(s, t, u)$  in the  $t$ -channel from the experimental  $\pi\text{-}\pi$  scattering results. This hope was illusory for the following reasons:

Above the  $\pi\pi \rightarrow K\bar{K}$  threshold unitarity quite fixes the both modulus and phase of the  $\pi\pi \rightarrow K\bar{K}$   $S$ -wave provided that the  $K\bar{K} \rightarrow K\bar{K}$   $S$ -wave phase shift is available, which is not the case.

Below the  $\pi\pi \rightarrow K\bar{K}$  threshold unitarity fixes the phase of the  $\pi\pi \rightarrow K\bar{K}$   $S$ -wave but does not yield any information about its modulus. Thus the exact determination of the  $\pi\text{-}\pi$  amplitude does not constrain in any way the modulus of the  $\pi\pi \rightarrow K\bar{K}$   $S$ -wave. Consequently in the region defined by  $|\cos \theta^*(t)| < 1$ , where a finite number of partial waves provides a good representation of the amplitude, only the phase of the complex zeros is determined, *i.e.*  $\text{Im} \cos \theta^*(t) / \text{Re} \cos \theta^*(t)$  and not the separate real and imaginary parts of  $\cos \theta^*(t)$ . For example, considering that this phase is nothing but the difference of the phases of  $I=0$   $S$ -wave and  $P$ -wave of the  $\pi\text{-}\pi$  scattering amplitude, we know that the complex zero of  $A(s, t, u)$  passes through the real  $(s, t, u)$ -plane for  $t \simeq 0.5$  (GeV)<sup>2</sup>, but we are unable to say where it does this on the straight line  $t = 0.5$  (GeV)<sup>2</sup>.

## 5. – Comparison of zero-contours in $\pi\text{-}\pi$ and $K\text{-}\pi$ scattering.

It is interesting to compare the zero-contours predicted by the simple Breit-Wigner model for  $\pi\text{-}\pi$  and  $K\text{-}\pi$  scattering. In both cases the nearby zero-contours are found to be simple closed curves which act as Adler-Weinberg zeros, zeros of  $P$ -wave resonance Legendre polynomials and double-pole-killing zeros. For the  $\pi\text{-}\pi$  amplitudes  $A_{\pi\pi}^{I=2}$  and  $A_{\pi\pi}^{I=1}$  the curves are circles (\*), whereas for the corresponding  $K\text{-}\pi$  amplitudes  $A(s, t, u)$  and  $B(s, t, u)$  the curves are ellipses (\*).

These zero-contour predictions, in spite of the very simple model from which they are drawn, appear to be in good agreement with the experimentally obtained contours of nearby zeros, at least for energies up to  $\simeq 0.95$  GeV. However, the prediction that the double-pole-killing zero and the upper branch

---

(\*) The  $\pi\text{-}\pi$  amplitude  $A_{\pi\pi}^{I=1}$  and the  $K\text{-}\pi$  amplitude  $B(s, t, u)$  are antisymmetric under the exchange  $s \leftrightarrow u$ , and they also possess a zero line for  $s = u$ .

of the contours form a single smooth curve fails for both  $\pi\text{-}\pi$  and  $\text{K}\text{-}\pi$  scattering, but for different reasons. In  $\pi\text{-}\pi$  scattering, due in part to the presence of the  $\text{S}^*$ -resonance situated between the  $\rho$  and  $\text{f}$ , the experimental contours of zeros remain well defined, with  $|\text{Im} \cos \theta^*(u)| \simeq 0.2$ , and it is clear that the « first »

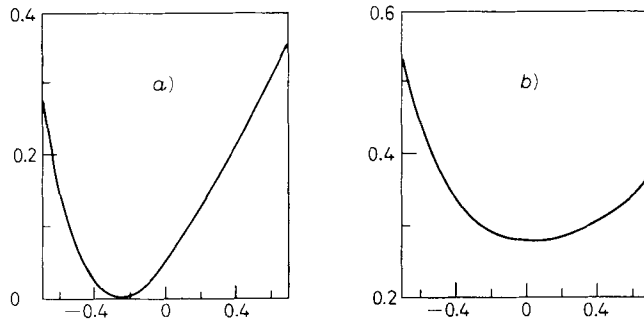


Fig. 8 - The differential cross-section (normalized to 1 for  $\cos \theta = -1$ ) vs.  $\cos \theta$  for a)  $\pi^+\pi^-\rightarrow\pi^+\pi^-$  at 1 GeV from the data of ref. (24), b)  $\text{K}^+\pi^-\rightarrow\text{K}^+\pi^-$  at 1.15 GeV from the data of ref. (12).

and « second » zero branches do not form a simple closed curve. On the other hand, in  $\text{K}\text{-}\pi$  scattering there are experimentally no nearby zeros in the energy range (0.95 ÷ 1.30) GeV, hence the concept of zero-contour is not well defined. However it is again clear that the model prediction of a closed curve of *nearby* zeros is not verified. In order to illustrate this difference we show in Fig. 8 the experimental differential cross-sections for  $\pi^+\pi^-$  (a) and  $\text{K}^+\pi^-$  (b) elastic scattering for energies approximately half-way between the  $\rho$  and  $\text{f}(a)$ , and between the  $\text{K}^*(890)$  and  $\text{K}^{**}(1420)$ . In case a) a pronounced minimum is visible, whereas the  $\text{K}\text{-}\pi$  cross-section has only a broad relatively poorly defined minimum.

## 6. - Summary.

We have shown that in the narrow-width  $\text{K}^*$  and  $\rho$  dominance model the zero-contour of the  $\text{K}\text{-}\pi$  amplitude  $A(s, t, u) = A^{t\text{-}\frac{1}{2}}(s, t, u)$  is a closed curve, an ellipse in the real  $(s, t, u)$ -plane. This curve fills three distinct roles: Adler-

---

(24) S. D. PROTOPODESCU, M. ALSTON-GARNJOST, A. BARBARO-GALTIERI, S. M. FLATTE, J. H. FRIEDMAN, T. A. LASINSKI, G. R. LYNCH, M. S. RABIN and F. T. SOLMITZ: *Conference on Meson Spectroscopy, Philadelphia, April 1972 (A.I.P. Conference Proceedings)*.

Weinberg zero inside the region below threshold in all channels,  $\rho$  and  $K^*$  Legendre zeros respectively in the  $t$ -channel near the  $\rho$  mass and in the  $u$ -channel physical region near the  $K^*$  mass, and double-pole-killing zero at the intersection of the lines  $t = m_\rho^2$  and  $u = m_{K^*}^2$ . The experimental zeros determined from the data of ref. (10-13) show clearly that the zero-contour is essentially that predicted by this simple model in the low-energy  $u$ -channel physical region ( $u \lesssim m_{K^*}^2$ ). This result lends support to the analysis of ARNEODO, GUERIN and DONOHUE (9), which emphasizes how, in the low-energy region ( $u \lesssim m_\rho^2$ ), unitarization gives rise to a very small distortion of the circular zero-contour given by the narrow-width  $\rho$  dominance approximation of the corresponding  $\pi$ - $\pi$  scattering amplitude  $A_{\pi\pi}^{I, m^2}(s, t, u)$ .

For the antisymmetric (under the exchange  $s \leftrightarrow u$ )  $K$ - $\pi$  amplitude  $B(s, t, u) = -A^{I, m^2}(s, t, u)/\sqrt{2}$  the narrow-width  $K^*$  and  $\rho$  dominance model predicts the zero-contour to consist of the line  $s = u$ , plus an ellipse passing through the Legendre zero of the  $K^*$  in the  $s$ - and  $u$ -channel physical regions and through both  $K^*$ - $\rho$  double poles. But this elliptic zero-contour is slightly more sensitive to unitarization at low energy ( $u \lesssim m_{K^*}^2$ ) than the elliptic zero-contour of the previous  $K$ - $\pi$  amplitude  $A(s, t, u)$ , and the experimental results show evidence for a possible contour of nearby zeros at  $t \simeq -0.2$  (GeV)<sup>2</sup>.

This model fails for  $u > m_{K^*}^2$ , since it predicts a closed contour of nearby zeros for the two  $K$ - $\pi$  amplitudes  $A(s, t, u)$  and  $B(s, t, u)$ , while experimentally the zeros have a nonnegligible imaginary part and that consequently the notion of zero-contour is not well defined at such energies. We must remark that the experimental zeros of the corresponding  $\pi$ - $\pi$  amplitudes (respectively  $A_{\pi\pi}^{I, m^2}$  and  $-A_{\pi\pi}^{I, m^2}/\sqrt{2}$ ) also disagree with the predictions of the narrow-width  $\rho$  dominance model, but not for the same reason, since they are well defined nearby zeros up to the  $f$  mass which do not propagate along the predicted circular curves for  $u > m_\rho^2$ .

It remains a puzzle why the simple Breit-Wigner model, which strongly violates unitarity, still predicts zero-contours in good agreement with experiment at low energy. The success of the analysis for  $\pi$ - $\pi$  scattering of PENNINGTON and SCHMID (8), which is based on the idea of zero-contours being relatively stable against unitarization, suggests that this idea may be of some phenomenological importance.

Finally we discussed how it was illusory to hope for the experimental definition of the paths of zeros of the  $K$ - $\pi$  scattering amplitude  $A(s, t, u)$  in the inelastic  $\pi\pi \rightarrow K\bar{K}$  channel, from the knowledge only of the exact features of the  $\pi$ - $\pi$  scattering amplitude.

\* \* \*

I would like to thank J. T. DONOHUE for reading the manuscript and interesting comments, and F. GUERIN for helpful discussions.

APPENDIX

**Kinematics and amplitudes in K- $\pi$  scattering.**

The conventional invariant variables of the elastic K- $\pi$  scattering

$$p_1 + p_1' \rightarrow p_2 + p_2'$$

are defined by

$$(A.1) \quad s = (p_1 + p_1')^2, \quad t = (p_1 - p_2)^2, \quad u = (p_1 - p_2')^2,$$

where  $p_1$  ( $p_2$ ) and  $p_1'$  ( $p_2'$ ) are the respective momenta of the incident (outgoing) pion and kaon. These variables obey the on-mass-shell relation

$$(A.2) \quad s + t + u = 2(\mu^2 + m^2),$$

with  $p_1^2 = p_2^2 = \mu^2$  and  $p_1'^2 = p_2'^2 = m^2$ .

In the  $s$ -channel c.m. system the outgoing momentum  $Q(s)$  and the scattering angle  $\theta(s)$  are given by

$$(A.3) \quad \begin{cases} Q(s) = \frac{1}{2} \sqrt{\frac{[s - (m + \mu)^2][s - (m - \mu)^2]}{s}}, \\ \cos \theta(s) = \left[ (t - u) + \frac{(m^2 - \mu^2)^2}{s} \right] / 4Q^2(s). \end{cases}$$

In the  $u$ -channel c.m. system the outgoing momentum  $Q(u)$  and the scattering angle  $\theta(u)$  are deduced from (A.3) by the exchange of the variables  $u$  and  $s$ .

In the  $t$ -channel the incoming momentum  $Q(t)$  and the scattering angle  $\theta(t)$  are given by

$$(A.4) \quad \begin{cases} Q(t) = \frac{1}{2} \sqrt{t - 4\mu^2}, \\ \cos \theta(t) = \frac{s - u}{\sqrt{t - 4\mu^2} \sqrt{t - 4m^2}}. \end{cases}$$

We use explicitly in this paper the convenient variables

$$(A.5) \quad q_s = \frac{1}{2} \sqrt{(m + \mu)^2 - s}, \quad q_u = \frac{1}{2} \sqrt{(m + \mu)^2 - u}, \quad q_t = \frac{1}{2} \sqrt{4\mu^2 - t}.$$

In our definition of zero-contours in Sect. 2, the limit one takes to approach the real  $(s, t, u)$ -plane corresponds to a particular prescription for these variables. For example, the  $(s + i0)$  limit corresponds to the prescription

$q_s = -i|q_s|$  for  $s$  real  $> (m + \mu)^2$ , the  $(s - i0)$  limit to  $q_s = i|q_s|$ . In the same way the  $(t + i0)$  limit corresponds to  $q_t = -i|q_t|$  for  $t$  real  $> 4\mu^2$ , the  $(t - i0)$  limit to  $q_t = i|q_t|$ .

The  $\mathbf{K}\text{-}\pi$  isospin amplitudes ( $I_s = \frac{1}{2}$  and  $\frac{3}{2}$ ) can be expressed in terms of two invariant amplitudes  $A^\pm(s, t, u)$  which exhibit definite crossing properties under  $s \leftrightarrow u$  exchange

$$(A.6) \quad \begin{cases} A^\pm(s, t, u) = \pm A^\pm(u, t, s), \\ A^{I-\frac{1}{2}}(s, t, u) = A^+(s, t, u) + 2A^-(s, t, u), \\ A^{I-\frac{3}{2}}(s, t, u) = A^+(s, t, u) - A^-(s, t, u). \end{cases}$$

The physical partial waves  $f_i^I(s)$  in the  $s$ -channel are defined by

$$(A.7) \quad f_i^I(s) = \frac{1}{2} \int_{-1}^{+1} A^I(s, t, u) P_i(\cos \theta(s)) d(\cos \theta(s))$$

with  $I = I_s$ . They are related to the elastic phase shifts  $\delta_i^I(s)$  through

$$(A.8) \quad f_i^I(s) = \frac{\sqrt{s}}{Q(s)} \exp[i\delta_i^I(s)] \sin \delta_i^I(s).$$

The scattering lengths are defined by

$$(A.9) \quad a_i^I = \lim_{s \rightarrow (m+\mu)^2} \left[ \frac{\delta_i^I(s)}{Q(s)^{2I+1}} \right],$$

which leads to the following  $S$ -wave scattering lengths

$$(A.10) \quad a_0^I = \frac{1}{(m + \mu)} f_0^I[(m + \mu)^2].$$

In the  $t$ -channel the inelastic process  $\pi\pi \rightarrow \mathbf{K}\bar{\mathbf{K}}$  is described by the amplitudes

$$(A.11) \quad \begin{cases} A^{I-\mathbf{0}}(t, s, u) = \sqrt{6} A^+(s, t, u), \\ A^{I-\mathbf{1}}(t, s, u) = 2A^-(s, t, u). \end{cases}$$

The physical partial waves  $T_i^I(t)$  are defined by

$$T_i^I(t) = \frac{1}{2} \int_{-1}^{+1} A^I(t, s, u) P_i(\cos \theta(t)) d(\cos \theta(t))$$

with  $I = I_t$ .